Int. J. Non-Linear Mechanics, Vol. 23, No. 3, pp. 231–239, 1988
Printed in Great Britain

0020–7462/88 $3.00 + 0.00
Pergamon Press plc

SUBHARMONIC ENTRAINMENT OF A FORCED RELAXATION OSCILLATOR

DUANE STORTI

Department of Mechanical Engineering, University of Washington, Seattle, WA 98195, U.S.A.

and

RICHARD H. RAND

Department of Theoretical and Applied Mechanics, Cornell University, Ithaca, NY 14853, U.S.A.

(*Received* 12 *May* 1987; *received for publication* 13 *October* 1987)

Abstract—Using a simplified model of a relaxation oscillator which exhibits the characteristic free response of intervals of slow decay separated by rapid jumps, we determine steady-state response to a harmonic forcing input and obtain regions in the parameter space where subharmonic entrainment occurs. The model relaxation oscillator consists of a one-dimensional flow with jump conditions and is motivated by earlier studies of the flow on the slow manifold of a piecewise-linear relaxation oscillator. The results are obtained by studying the dynamics of the phase mapping which describes how the forcing phase varies between jumps. Details of the phase mapping are obtained both analytically and by numerical integration of the governing flow. The results obtained regarding existence and stability of subharmonics bear strong qualitative resemblance to experimental observations of frequency demultiplication by van der Pol and van der Mark (1927) and to numerical investigations of the forced van der Pol oscillator by Flaherty and Hoppensteadt (1978).

INTRODUCTION

The phenomenon of subharmonic entrainment of a relaxation oscillator by a periodic forcing function was first investigated by van der Pol and van der Mark [1]. They found experimentally that when a certain electric circuit (a relaxation oscillator) is forced with a sinusoidally-varying voltage, "the system is only capable of oscillating with discrete frequencies, these being determined by whole submultiples of the applied frequencies". They called this phenomenon "frequency demultiplication".

The phenomenon may be described as follows: if the frequency of the forcer is exactly (an integer) M times the frequency of the unforced (limit cycle) frequency of the relaxation oscillator, we may expect a subharmonic of order M to occur. If the frequency of the forcer is then increased (decreased) to be slightly larger (smaller) than M times the unforced frequency, the subharmonic of order M will still persist. If, however, the forcing frequency is increased (decreased) sufficiently, the system will exhibit a higher (lower) order subharmonic.

The purpose of this paper is to offer a simplified model of this phenomenon, and to obtain from the model an understanding of which subharmonics occur in various regions of the parameter space.

THE MODEL

The usual mathematical model for the forced relaxation oscillator is the van der Pol equation which, following Levi's [2] notation, is given by

$$\varepsilon x'' + \varphi_{\mathrm{vdp}}(x)x' + \varepsilon x = b\cos t \tag{1}$$

where primes indicate differentiation with respect to the independent variable (time), b is the forcing amplitude, ε is a small parameter, and $\varphi_{\mathrm{vdp}} = x^2 - 1$ can be interpreted as a variable damping coefficient accounting for the system's non-linearity. While similar systems (i.e. periodically forced relaxation oscillators) have been studied both analytically and numerically by Cartwright and Littlewood [3], Flaherty and Hoppensteadt [4], Grasman *et al.* [5], we will be most interested in following up on a simplification introduced

by Levinson [6] whereby the damping coefficient is instead taken to be a piecewise constant function of the dependent variable, i.e.

$$\varphi(x) = \begin{cases} 1, & |x| > 1 \\ -1, & |x| < 1. \end{cases} \tag{2}$$

Levinson [6] and Levi [2] have shown that this simplifies the analysis of the forced relaxation oscillator without causing significant qualitative changes in the behavior of the system. A similar piecewise constant version of $\varphi(x)$ shown in Fig. 1 has been employed by Belair and Holmes [7] and Storti and Rand [8] to study the dynamics of coupled relaxation oscillators.

The forced relaxation oscillator can be expressed as a system of two first order differential equations in terms of Lienard variables as follows (see Minorsky, [9]):

$$u' = -\varepsilon x + b\cos t \tag{3}$$

$$x' = [u - \Phi(x)]/\varepsilon \tag{4}$$

where

$$\Phi(x) = \int_0^x \varphi(x)x'\,dt = \int_0^x \varphi(x)\,dx = \begin{cases} x-2, & x > 1 \\ -x, & -1 < x < 1 \\ x+2, & x < -1 \end{cases} \tag{5}$$

and u is defined [from equation (4)] as

$$u = \varepsilon x' + \int_0^x \varphi(x)\,dx. \tag{6}$$

Levi [2] observes that the presence of the small parameter in the denominator of equation (4) indicates the existence of a slow manifold associated with the curve $u = \Phi(x)$ as seen in Fig. 2 which depicts the phase plane for the unforced relaxation oscillator. The flow contracts strongly toward the stable branches ($|x| > 1$) of the slow manifold. Along the stable branches of the slow manifold, the flow consists of a sinusoidal oscillation superposed on a slow drift (downwards for $x > 1$ and upwards for $x < -1$). As a trajectory drifts past the endpoint ($x = \pm 1$) of a stable branch of the slow manifold, the fast flow takes over and rapidly brings the trajectory into the vicinity of the other stable branch along a nearly horizontal path. A more detailed description of the phase portrait is given by Belair and Holmes [7] and Storti and Rand [8]. Motivated by this behavior, we propose a simplified

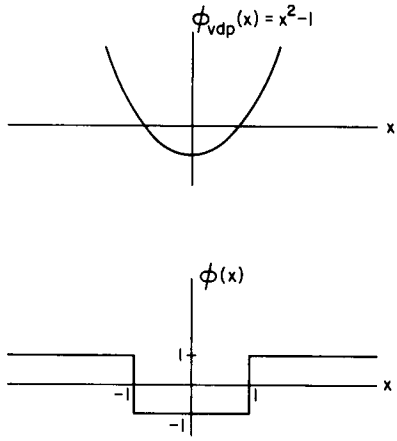

Fig. 1. Variable damping coefficients for relaxation oscillators: (a) van der Pol and (b) simplified.

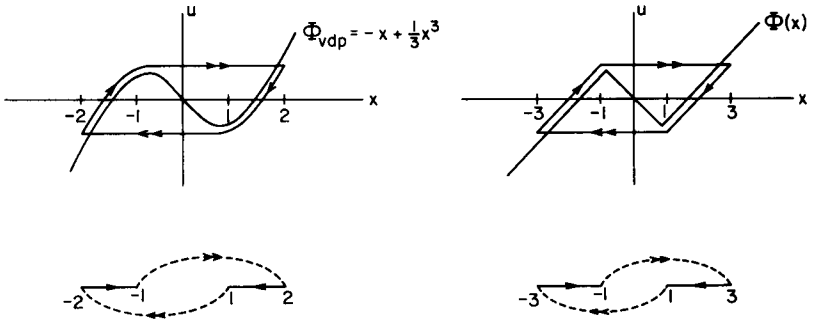

Fig. 2. Phase portraits for the unforced relaxation oscillators showing projection of the limit cycle onto the x-axis: (a) van der Pol and (b) simplified. Single arrows represent flow along the slow manifold. Double arrows represent fast flow which we model as an instantaneous jump.

relaxation oscillator where the fast horizontal flow is replaced by an instantaneous jump, and the flow is otherwise restricted to the stable branches of the slow manifold. This simplified relaxation oscillator is governed by the flow of a single first order differential equation

$$x' = -\varepsilon x + b\cos t \tag{7}$$

[obtained from equation (3) by noting that $u' = x'$ on the stable branches of the slow manifold] and the jump condition $x = \pm 1 \to x = \mp 3$, as indicated in the lower portion of Fig. 2 where the limit cycle is projected onto the x-axis. Further simplification can be achieved by noting that the flow is invariant under the transformation $(x, t) \to (-x, t - \pi)$ and the dynamics of the system can be studied by considering the flow of equation (7) on $x > 1$ with the jump/time-reset condition $x(t_1) = 1 \to x(t_1 - \pi) = 3$.

ANALYSIS OF THE MODEL

To determine the steady-state behavior of the relaxation oscillator, we begin by investigating how solutions decay from the landing point ($x = 3$) to the jump point ($x = 1$). Applying the initial condition $x(t_0) = 3$ specifies the following solution of equation (7)

$$x(t; t_0) = \left[3 - \frac{b}{1+\varepsilon^2}(\sin t_0 + \varepsilon\cos t_0)\right]e^{-\varepsilon(t-t_0)} + \frac{b}{1+\varepsilon^2}(\sin t + \varepsilon\cos t) \tag{8}$$

which in terms of $\tau = t + \tan^{-1}\varepsilon$ and $B = b(1+\varepsilon^2)^{-1/2}$ has the simpler form

$$x(\tau; \tau_0) = [3 - B\sin\tau_0]e^{-\varepsilon(\tau-\tau_0)} + B\sin\tau. \tag{9}$$

Note that the behavior of x is as described earlier: a sinusoidal oscillation of magnitude B superposed on an exponential decay at rate ε. Figure 3 shows the trajectory $x(\tau; \tau_0)$ for three values of the initial phase τ_0 with $\varepsilon = 0.02$ and $b = 0.5$. The jump time τ_1 [the smallest $\tau > \tau_0$ for which $x(\tau; \tau_0) = 1$] is a single-valued function of τ_0 implicitly given by

$$[3 - B\sin\tau_0]e^{-\varepsilon(\tau_1-\tau_0)} + B\sin\tau_1 = 1. \tag{10}$$

From Fig. 3 it is clear that the function $\tau_1(\tau_0)$ will generally involve discontinuities, the number and location of which depend on the parameters B and ε.

The forcing phase $\psi = \psi(\tau_0)$ at the jump time is defined by

$$\psi = \tau_1 - N \tag{11}$$

where $N = \text{int}(\tau_1/2\pi)$ so that $0 < \psi < 2\pi$. Periodic subharmonic solutions of order $M = 2N + 1$ (i.e. with period $[(2N+1)2\pi]$) arise when the flow from $x(\tau_0) = 3$ to $x(\tau_1) = 1$

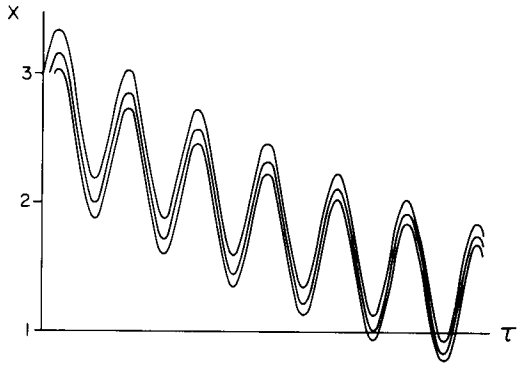

Fig. 3. Sample trajectories for various values of initial phase with $\varepsilon = 0.02$, $b = 0.5$. The upper, middle and lower curves correspond to initial phase $\tau_0 = 0.1$, 0.6 and 1.1 respectively. These trajectories cease to be valid when x first becomes unity, after which the jump occurs. Note that the jump time for the upper curve is substantially longer than those for the lower curves despite a relatively small change in initial forcing phase.

composed with a jump to $x(\tau_1 - \pi) = 3$ returns the original phase, i.e.

$$f(\tau_0) = \psi(\tau_0) - \pi = \tau_0. \tag{12}$$

The function $f: [-\pi, \pi] \to [-\pi, \pi]$ will be referred to as the phase mapping and its fixed points correspond to periodic solutions for the relaxation oscillator. Thus we may study the behaviour of the system by considering the dynamics obtained by iterating the map f.

Figure 4 shows an example of a phase mapping determined by numerical integration of (7) with parameter values $\varepsilon = 0.02$, $b = 0.5$. Fixed points are determined by intersections of the phase map with the 45° line. The example shown is typical of those throughout much of the parameter space in that the map lies in a strip just below $f = \pi/2$, consists of several branches associated with different values of N (as labeled), and has no more than two fixed points. We will return later to consider the existence and stability of fixed points analytically, but for now let us continue with the numerical results. By obtaining phase maps over a range of decay rates (i.e. over a range of periods for the unforced relaxation oscillator), locating the fixed points, and noting the corresponding order of the associated subharmonic, we obtain a plot of N vs ε as shown in Fig. 5. As the decay rate ε is increased (or the unforced period is decreased), there are alternating intervals with one or two stable periodic orbits. In the intervals with two stable periodic orbits, their periods are distinct, i.e. subharmonics of different orders coexist. If ε is then decreased, hysteresis loops indicated by dashed vertical lines are observed. This figure bears striking resemblance to the experimental results of van der Pol and van der Mark [1] and the numerical results of

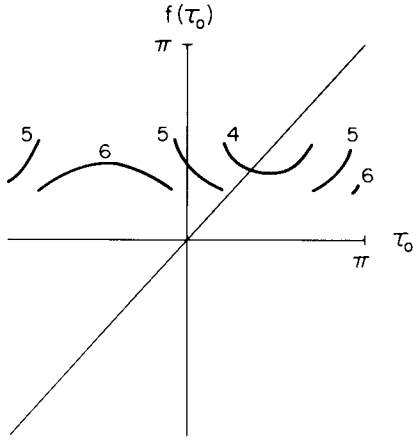

Fig. 4. Sample phase map with parameter values $\varepsilon = 0.02$, $b = 0.5$. The value of N associated with each branch is indicated, cf. Fig. 3.

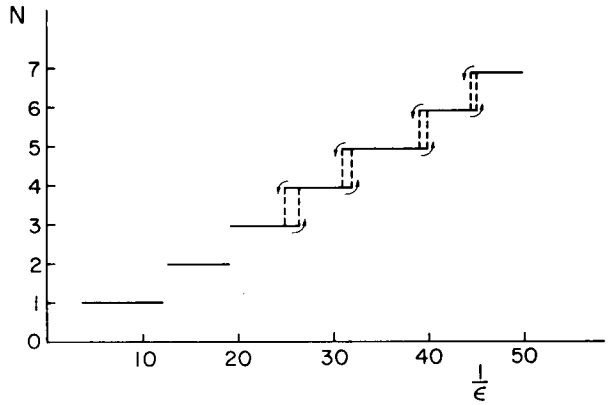

Fig. 5. Plot of N vs ε^{-1} with $b = 0.20$ showing entrainment and coexistence. Note that the period of the response is $(2N + 1)2\pi$ and the period of the unforced relaxation oscillator is $2 \ln 3/\varepsilon$ [which follows from equation (10) with $b = 0$].

Flaherty and Hoppendsteadt ([4], Fig. 3).

Repeating this sort of numerical study for a sequence of values of forcing amplitude, we obtain the regions in the b, ε plane where subharmonics of order $M = 2N + 1$ occur. These regions are shown in Fig. 6 and they closely resemble the regions obtained by Flaherty and Hoppensteadt ([4], Fig. 2) for subharmonic entrainment of the van der Pol oscillator in the region $0 \leq \varepsilon < 0.14$, $0 \leq b < 0.5$. There are no regions with more than two stable periodic orbits, and there is a sequence of wedges near the ε-axis where no periodic orbits are observed, corresponding to the noisy gaps reported in [1].

Note from Fig. 6 that the model is particularly sensitive to parameter changes near the point $b = 1$, $\varepsilon = 0$; i.e. large changes in the order of the subharmonics can result from slight variations of the parameters.

To further understand the dynamics of this system, an analytical investigation, described in the Appendix, was undertaken which leads to the following equations for the lower and upper bounds for the regions in the ε, b plane where subharmonics of order $M = 2N + 1$ can occur:

$$b_{L,N}(\varepsilon) = \left| 3 - \frac{4}{1 + e^{-\varepsilon(2N+1)\pi}} \right| \tag{13}$$

$$b_{U,N}(\varepsilon) = \left(\frac{1}{1 - 2\pi\varepsilon} \right) \left[3 + 2\pi\varepsilon - \frac{4}{1 + e^{-\pi\varepsilon(2N+3)}} \right]. \tag{14}$$

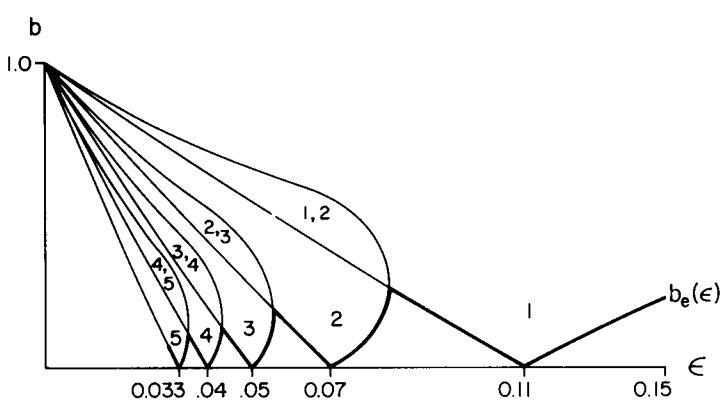

Fig. 6. Subharmonic entrainment regions obtained by numerical evaluation of phase maps. Numbers shown indicate possible values of N.

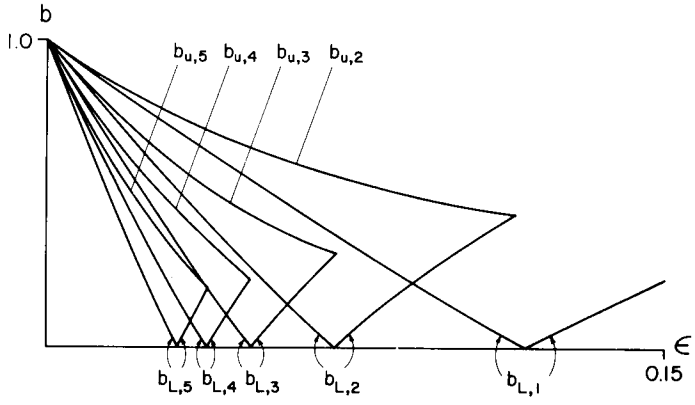

Fig. 7. Analytic bounds on entrainment regions from equations (13) and (14).

These curves are plotted for various values of N in Fig. 7. The analytically determined entrainment regions agree closely with the numerically determined regions, but, due to the approximate nature of the upper bounds, are somewhat conservative when εN becomes large. A detailed derivation of the bounding curves, as well as an examination of the characteristics of the phase mapping, its fixed points and their stability is contained in the Appendix for the interested reader.

CONCLUSION

We have presented and analyzed a simplified model for the periodic response of a sinusoidally forced relaxation oscillator. Both numerical and analytic results indicate that the model qualitatively captures the essential subharmonic entrainment phenomenon exhibited by the van der Pol relaxation oscillator. Some of the more complicated dynamics, discussed in detail in [2] are lost by the model, but it has the redeeming feature that it is governed by a single ordinary differential equation with jump conditions. Thus the simplified relaxation oscillator lends itself to relatively rapid numerical simulation which would be especially desirable in the study of forced systems of many coupled oscillators. Models of this type have already been applied with some success in determining existence and stability of phase-locked modes in systems of two relaxation oscillators by Storti [10], Storti and Rand [8], Belair and Holmes [7]. It was found that although the simplified model did reflect most of the qualitative features of the full (4th order) system, some of the dynamics were lost by the model due to sensitivity of stability to changes in the shape of the limit cycle arising from the instantaneous jump assumption, see Storti [10], Storti and Rand [11].

Acknowledgment—The first author's work was partially supported by National Science Foundation grant #CBT-8504973. The second author was partially supported by grants from the National Science Foundation, the Army Research Office through the Mathematical Sciences Institute, and the Air Force Office of Scientific Research. We wish to express our thanks to these organizations for their support and to Mr Tu Luc Nguyen for his assistance in performing the numerical aspects of this investigation.

REFERENCES

1. B. van der Pol and J. van der Mark, Frequency demultiplication. *Nature* **120**, 363–364 (1927).
2. M. Levi, Qualitative analysis of the periodically forced relaxation oscillations. *Memoirs AMS* **244**, (1981).
3. M. L. Cartwright and J. E. Littlewood, On non-linear differential equations of the second order: I. The equation $y'' - k(1 - y^2)y' + y = b\lambda t + \alpha$, k large. *J. London math. Soc.* **20**, 180–189 (1945).
4. J. E. Flaherty and F. C. Hoppensteadt, Frequency entrainment of a forced van der Pol oscillator. *Studies appl Math.* **58**, 5–15 (1978).
5. J. Grasman, E. J. M. Veling and G. M. Willems, Relaxation oscillations governed by a van der Pol equation. *SIAM J appl. Math.* **31**, 667–676 (1976).
6. N. Levinson, A second-order differential equation with singular solutions. *Ann. Math.* **50**, 127–153 (1949).
7. J. Belair and P. Holmes, On linearly coupled relaxation oscillators, *Q. appl. Math.* **42**, 193–219 (1984).
8. D. Storti and R. Rand, Dynamics of two strongly coupled van der Pol oscillators. *Int. J. Non-linear Mech.* **17**, 143–152 (1982).
9. N. Minorsky, *Nonlinear oscillations*, p. 109. Krieger, New York (1974).

10. D. Storti, *Coupled relaxation oscillators: stability of phase-locked modes*, Ph.D. Thesis, Cornell University, Ithaca, NY (1984).
11. D. Storti and R. Rand, Dynamics of two strongly coupled relaxation oscillators. *SIAM J. appl. Math.* **46**, 56–67 (1986).
12. P. Berge, Y. Pomeau and C. Vidal, *Order within Chaos: Towards a Deterministic Approach to Turbulence*, John Wiley, New York (1984).
13. D. Storti and R. Rand, A simplified model of coupled relaxation oscillators, *Int. J. Non-Linear Mech.* **22**, 283–289 (1987).

APPENDIX

For further information regarding the number and stability of fixed points, we return to the analytical study of the solutions of the governing equation. Substituting the periodicity requirement $\tau_1 = \tau_0 + (2N+1)\pi$ into (9), we obtain an expression for the initial phase associated with a subharmonic of order $M\ (= 2N+1)$

$$\tau_0 = \sin^{-1}\left[\frac{1}{B}\left(3 - \frac{4}{1+e^{-\varepsilon(2N+1)\pi}}\right)\right]. \tag{A1}$$

This locates the fixed points of f, but we must determine which values of N are relevant. Some limits can be determined by noting restrictions on the argument of $\sin^{-1}$ in equation (A1). Since we are interested in real values of τ_0, the argument must have absolute value no greater than unity. This leads to a series of curves in the ε, b plane, described by equation (13), above which fixed points of order M can exist. Beneath these curves, shown in Fig. 7, there are a series of wedge-shaped regions, nearly identical to those in Fig. 6, in which no fixed points exist. The jagged curve bounding the wedges is labeled $b_e(\varepsilon)$ (e stands for entrainment) since it gives the minimum amplitude for which the forcer can entrain the relaxation oscillator to respond at a submultiple of the forcing frequency. For $b < b_e$, the phase relationship is drifting. As the forcing amplitude increases through b_e, a stable fixed point arises due to a tangent bifurcation. As the forcing amplitude approaches b_e from below, the phase map comes nearly into contact with the 45° line and the phase drift becomes very slow in this vicinity. Thus the phase at the jump remains nearly constant for a large number of iterations, then changes rapidly over a few cycles until it returns near the phase associated with the slow drift. The number of iterations between large phase changes goes to infinity as $b \to b_e$ and phase locking occurs. This mechanism for transition from disordered (drifting) to ordered (periodic) behavior, known as intermittency, is described more fully by Berge *et al.* [12].

The other curve bounding a region comes from the lower limit on the argument of $\sin^{-1}$ in equation (A1). From the example phase map of Fig. 4, we see that the smallest value of the final phase $f(\tau_0)$ is associated with the initial phases where the discontinuities in the phase map occur. Figure 3 illustrates that the discontinuities in $f(\tau_0)$ occur when a trajectory's first contact with the jump line ($x = 1$) is a tangency instead of a transverse intersection, i.e. $x'(\tau_1^*; \tau_0^*) = 0$. A small change in τ_0 can then destroy the contact causing the jump time τ_1 to increase by Δ to $\tau_1^{**} = \tau_1^* + \Delta$. Since τ_1^* is the jump time, we have [from equation (9)]

$$[3 - B\sin\tau_0^*]\,e^{-\varepsilon(\tau_1^* - \tau_0^*)} + B\sin\tau_1^* = 1 \tag{A2}$$

and the tangency condition gives [differentiating equation (9)]

$$-[3 - B\sin\tau_0^*]\,\varepsilon e^{-\varepsilon(\tau_1^* - \tau_0^*)} + B\cos\tau_1^* = 0. \tag{A3}$$

Eliminating τ_0^* yields

$$\cos\tau_1^* + \varepsilon\sin\tau_1^* = \varepsilon/B \tag{A4}$$

or

$$\tau_1^* = \tan^{-1}\varepsilon + \cos^{-1}[\varepsilon/b] \tag{A5}$$

which can only be satisfied for real values of τ_1^* if $b > b_c = \varepsilon$ (or equivalently $B \geqslant B_c = \varepsilon[1+\varepsilon^2]^{-1/2}$). An expression for the size of the discontinuity, Δ, can be obtained by noting that the point $(\tau_1^* + \Delta, 1)$ lies on a solution of equation (7) passing through $(\tau_1^*, 1)$. Therefore

$$[1 - B\sin(\tau_1^* + \Delta)]e^{\varepsilon\Delta} + B\sin\tau_1^* = 1 \tag{A6}$$

and substituting the expression for $\tau_1^*(\varepsilon, b)$ found previously [in equations (A4) and (A5)] gives

$$1 + \varepsilon^2 - \left[\varepsilon^2 - \sqrt{b^2 - \varepsilon^2}\right]\cos\Delta + \varepsilon\left[1 + \sqrt{b^2 - \varepsilon^2}\right]\sin\Delta = e^{-\varepsilon\Delta}\left[1 + \sqrt{b^2 - \varepsilon^2}\right]. \tag{A7}$$

While this expression is quite complicated, one conclusion can be drawn from it immediately. Since N does not appear, the change in the value of f at each discontinuity is the same. More information can be obtained by using an approximate analysis to consider the case $\varepsilon \ll b = 0(1)$ which is of interest for relaxation oscillations. Neglecting terms of order ε^2 gives

$$1 + b = (1 + \varepsilon\Delta)\left[1 + b\cos\Delta + \varepsilon\left(1 + \frac{1}{b}\right)\sin\Delta\right]. \tag{A8}$$

We look for an approximate solution for Δ of the form

$$\Delta = \Delta_0 + g_1(\varepsilon)\Delta_1 + \ldots, \qquad \text{where } g_1(\varepsilon) = o(1). \tag{A9}$$

Substituting into equation (A8) and retaining terms of order ε^0 gives

$$1 + b = 1 + b\cos\Delta_0 \tag{A10}$$

which is satisfied when $\cos\Delta_0 = 0$. Since the time between a tangency and the next intersection with the jump line approaches one full forcing cycle as $\varepsilon \to 0$ and the exponential decay disappears, the correct value is $\Delta_0 = 2\pi$. Substituting again into equation (A6) and retaining leading order terms gives

$$1 + b = (1 + 2\pi\varepsilon + \varepsilon g_1(\varepsilon)\Delta_1)\{1 + b[1 - (g_1(\varepsilon)\Delta_1)^2/2] + (b + 1)\varepsilon g_1(\varepsilon)\Delta_1/b\} + \ldots . \tag{A11}$$

Canceling the $O(1)$ terms and neglecting terms of order $\varepsilon g_1(\varepsilon)$ compared with those of order ε, we obtain

$$0 = \varepsilon 2\pi(1 + b) - b g_1^2(\varepsilon)\Delta_1^2/2 \tag{A12}$$

which is satisfied when $g_1(\varepsilon) = \varepsilon^{1/2}$ and $\Delta_1 = \pm 2[(b + 1)\pi/b]^{1/2}$. Taking the negative root (since Δ must not exceed 2π) yields

$$\Delta = 2\pi - 2[(1 + b)\pi\varepsilon/b]^{1/2} + o(\varepsilon^{1/2}). \tag{A13}$$

Expanding equation (A6) for small ε gives an approximate expression for the forcing phase at the tangency: $\tau_1^* = 3\pi/2 + O(\varepsilon)$. Since $f(\tau_0) = \tau_1 - \pi$, this says that to order ε the phase map achieves a maximum value of $\pi/2$ then jumps down to a value $\pi/2 - h$ where $h = 2\pi - \Delta$. This corroborates the numerical evidence that the phase map lies in a strip just below $\pi/2$. In addition, we can now estimate the height of the strip by $h = 2[(1 + b)\pi\varepsilon/b]^{1/2} + O(\varepsilon)$.

The other curve bounding an entrainment region comes from our knowledge of the position of the lower edge of the strip; i.e. $\tau_0 \geq \pi/2 - h$. Substituting the minimum value of $\tau_0 (= -h + \pi/2)$ into equation (A1) and replacing N by $N + 1$ (since the subharmonic disappears after the corresponding fixed point has moved to the second lowest order branch of the phase map) yields the upper bound

$$b_{U,N}(\varepsilon) = \left(\frac{1}{1 - 2\pi\varepsilon}\right)\left[3 + 2\pi\varepsilon - \frac{4}{1 + e^{-\pi\varepsilon(2N+3)}}\right]. \tag{A14}$$

To establish this as a reasonable upper bound for b, we must show that no more than two fixed points can coexist. To do this, consider the "worst case" when the phase map has a fixed point at $\tau_0 = \pi/2$ so that the lowest order (N) branch of the phase map consists of this single point. The next lowest branch of the phase map, which may contain a second fixed point, extends continuously backwards from a value of $\pi/2 - h$ at $\tau_0 = \pi/2^-$ to a value of $\pi/2$ at $\tau_0 = \tau_0^{\#}$ where the next discontinuity occurs. We will show that $\tau_0^{\#}$ lies outside the interval $[\pi/2 - h, \pi/2]$ where fixed points may exist. This fact can be observed directly from Fig. 8. Curve A shows the trajectory originating from $\tau_0^* = \pi/2$. It has a tangency with the jump line $x = 1$ at τ_1^* and intersects the jump line transversely at $\tau_1^{**} = \tau_1^* + \Delta = \tau_1^* + 2\pi - h$. Curve B shows the trajectory originating at $\tau_0^{\#}$. The dashed curve C is obtained by raising curve A vertically so that it coincides with curve B at $\tau_1^{\#} = \tau_1^* + 2\pi$. From the figure it is clear that $\tau_0^{\#} < \pi/2 - h$, indicating that no more than two periodic orbits can coexist.

The upper bounds on forcing amplitude allowing for a given subharmonic are shown as the upper edge of the regions in Fig. 7. Comparison with the numerical results of Fig. 6 indicate that these bounds are reasonable, but somewhat conservative toward the right-hand side of the region.

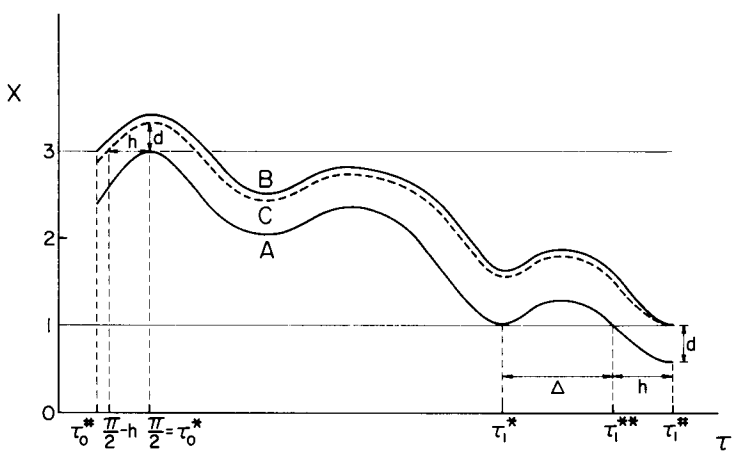

Fig. 8. Sketch of trajectories which have tangencies with the jump line.

Finally, we compute the derivative of the map $f(\tau_0)$ from equations (10)–(12)

$$\frac{df(\tau_0)}{d\tau_0} = \frac{[B\cos\tau_0 - \varepsilon(3 - B\sin\tau_0)]e^{-\varepsilon(\tau_1 - \tau_0)}}{B\cos\tau_1 - \varepsilon(3 - B\sin\tau_0)e^{-\varepsilon(\tau_1 - \tau_0)}} \tag{A15}$$

neglect terms of order ε, and evaluate at the fixed points to obtain

$$\left[\frac{df}{d\tau_0}\right]_{\tau_0 = f(\tau_0)} = -e^{-\varepsilon(\tau_1 - \tau_0)} + \dots . \tag{A16}$$

Thus the derivative evaluated at a fixed point has magnitude less than unity, and all of the fixed points discussed are stable (for $\varepsilon \ll 1$).